Pergamon

Acta mater. 49 (2001) 2645–2652

Acta MATERIALIA

www.elsevier.com/locate/actamat

HIGH-STRENGTH Cu-BASED BULK GLASSY ALLOYS IN Cu–Zr–Ti AND Cu–Hf–Ti TERNARY SYSTEMS

A. INOUE[1,2], W. ZHANG[2], T. ZHANG[1]† and K. KUROSAKA[3]

[1]Institute for Materials Research, Tohoku University, Sendai 980-8577, Japan, [2]Inoue Superliquid Glass Project, Exploratory Research for Advanced Technology, Japan Science and Technology Corporation, Sendai 982-0807, Japan and [3]Graduate School, Tohoku University, Sendai 980-8577, Japan

(Received 15 March 2001; received in revised form 22 March 2001; accepted 1 May 2001)

Abstract—New Cu-based bulk glassy alloys were formed in Cu–Zr–Ti and Cu–Hf–Ti systems by the copper mold casting method. The critical diameter is 4 mm for the $Cu_{60}Zr_{30}Ti_{10}$ and $Cu_{60}Hf_{25}Ti_{15}$ alloys which are larger than 1 mm for the $Cu_{60}Zr_{40}$ and $Cu_{60}Hf_{40}$ glassy alloys. The substitution of Zr or Hf for Ti causes an increase in the glass-forming ability (GFA). As the Ti content increases, the glass transition temperature (T_g), crystallization temperature (T_x), and the supercooled liquid region $\Delta T_x(= T_x - T_g)$ decrease for both $Cu_{60}Zr_{40-x}Ti_x$ and $Cu_{60}Hf_{40-x}Ti_x$ alloys. In contrast, the liquid temperature (T_l) has a minimum value of 1127 K for the $Cu_{60}Zr_{20}Ti_{20}$ alloy and 1175 K for the $Cu_{60}Hf_{20}Ti_{20}$ alloy, resulting in a maximum T_g/T_l of 0.63 and 0.62, respectively. The alloys with the highest T_g/T_l value showed the highest GFA for these Cu-based alloys. The bulk glassy alloys exhibit high tensile fracture strength of 2000–2160 MPa, compressive fracture strength of 2060–2150 MPa and compressive plastic elongations of 0.8–1.7%. The finding of the new Cu-based bulk glassy alloys with high GFA, high fracture strength above 2000 MPa and distinct plastic elongation is encouraging for the future development of a new type of bulk glassy alloy which can be used for structural materials.

Keywords: Casting; Stress–strain relationship measurements; Metallic glasses; Mechanical properties; Phase transformations

1. INTRODUCTION

Since the first synthesis of a La–Al–Ni bulk glassy alloy by copper mold casting in 1989 [1], a number of bulk glassy alloys have been reported in multi-component systems such as Mg [2], Zr [3, 4], Ti [5], Fe [6], Pd–Cu [7], Ni [8] and Co [9] based alloys. Although these alloy systems with high glass-forming ability are extended to quaternary, pentad and more multicomponent systems, it is important to search for a new ternary glassy alloy system, because a number of previous results indicated that addition of a small amount of other element to simple ternary systems enhances the glass-forming ability [10–12]. So far, there have been no reports on the formation of a bulk glassy alloy in Cu-based alloys containing more than 50 at.% Cu, though some bulk glassy alloys have been obtained in Cu–Ti–Zr–Ni [13], Cu–Ti–Zr–Ni–Si [14] and Cu–Ti–Zr–Ni–Sn [15] systems containing Cu less than 40 at.%. Very recently, we have found that bulk glassy alloys with a thickness of 4 mm are formed in Cu–Zr–Ti [16] and Cu–Hf–Ti ternary and Cu–Zr–Hf–Ti quaternary systems and these exhibit good mechanical properties. The development of Cu-based bulk glassy alloys is important to extend the applications of bulk metallic glasses. This paper presents the composition range in which a glassy phase is formed in the Cu–Zr–Ti and Cu–Hf–Ti systems by copper mold casting and the compositional dependence of the thermal stability and the mechanical properties of the bulk glassy alloys. In addition, the reason for the high glass-forming ability in these ternary systems is discussed.

2. EXPERIMENTAL PROCEDURE

Ternary alloys in Cu–Zr–Ti and Cu–Hf–Ti systems were prepared by arc melting the mixtures of pure Cu, Zr, Hf and Ti metals in an argon atmosphere. Ribbon samples with a cross section of 0.02×1.2 mm^2 were prepared by the melt spinning technique. Bulk alloys in a cylindrical form with a length of 70 mm and diameters up to 7 mm were prepared by the copper mold casting method. In addition, bulk sheets of dimension $30 \times 70 \times 2$ mm^3 were also prepared by the mold-clamp casting technique [17, 18]. Glassy struc-

† To whom all correspondence should be addressed. Tel.: +81-22-215-2199; Fax: +81-22-215-3047.

E-mail address: zyc@mail.cc.tohoku.ac.jp (T. Zhang)

1359-6454/01/$20.00
PII: S1359-6454(01)00181-1

ture was identified by X-ray diffraction and optical microscopy (OM). Thermal stability associated with the glass transition temperature (T_g) and crystallization temperature (T_x) was examined by differential scanning calorimetry at a heating rate of 0.67 K/s. The melting and liquid temperatures were determined by differential thermal analysis (DTA) at a heating rate of 0.17 K/s. Mechanical properties under tensile and compressive deformation modes were measured at room temperature with an Instron-type testing machine. The Young's modulus was measured using a strain-gauge meter. Fracture surface was examined by scanning electron microscopy (SEM).

3. RESULTS

3.1. Thermal stability of supercooled liquid

It has previously been reported that a glassy phase in Cu–Zr and Cu–Hf binary systems is formed in wide composition ranges of 30–70 at.% Zr or Hf [19]. Figures 1 and 2 show the differential scanning calorimetric (DSC) curves of the melt-spun $Cu_{100-x}Zr_x$ and $Cu_{100-x}Hf_x$ (x = 30–70 at.%) binary glassy alloys, respectively. Although no glass transition is observed for the 30% Zr and 30% Hf alloys, a further increase in Zr or Hf content results in the appearance of distinct glass transition, followed by a large supercooled liquid region. T_g and T_x tend to decrease monotonically with increasing Zr or Hf content, although the melting temperatures of Zr and Hf metals are much

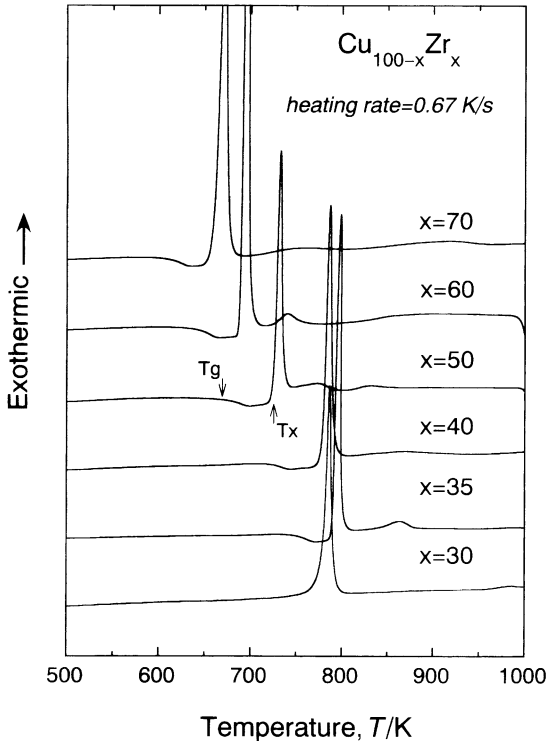

Fig. 1. DSC curves of melt-spun $Cu_{100-x}Zr_x$ (x = 30–70 at.%) glassy alloys.

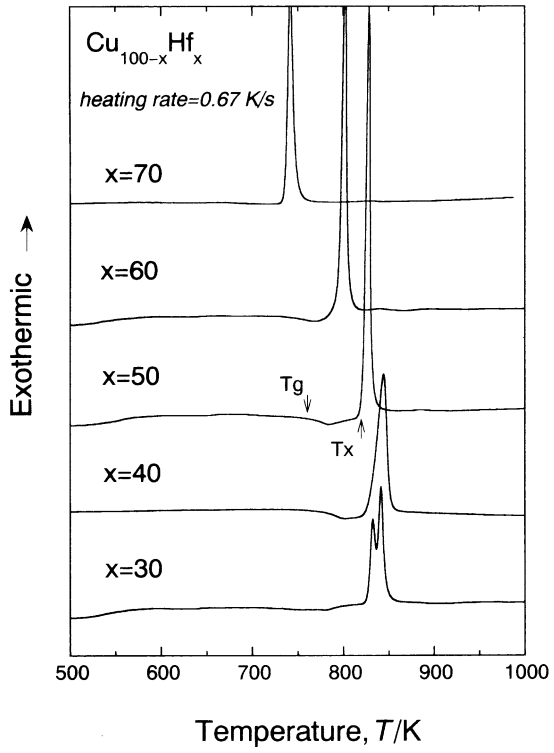

Fig. 2. DSC curves of melt-spun $Cu_{100-x}Hf_x$ (x = 30–70 at.%) glassy alloys.

higher than that of Cu metal. It is also seen that the supercooled liquid region defined by the temperature interval between T_g and T_x, ΔT_x ($= T_x - T_g$) shows maximum values of 55 K at 40 at.% Zr and 59 K at 50 at.% Hf, and then decreases gradually as it deviates from these compositions. The crystallization of the 40% Zr or 50% Hf alloy with the largest supercooled liquid region takes place through a single exothermic reaction. It is confirmed that the exothermic reaction is due to the precipitation of the Cu_3Zr_2 phase for the $Cu_{60}Zr_{40}$ alloy and the $Cu_3Hf + CuHf_2$ phases for the $Cu_{50}Hf_{50}$ alloy.

Subsequently, we examined the effect of Ti addition on the glass transition and the thermal stability of the supercooled liquid region in the alloy series of $Cu_{60}Zr_{40-x}Ti_x$ and $Cu_{60}Hf_{40-x}Ti_x$. Figures 3 and 4 show the DSC curves of the melt-spun $Cu_{60}Zr_{40-x}Ti_x$ and $Cu_{60}Hf_{40-x}Ti_x$ (x = 0–40 at.%) alloys, respectively. In comparison with the $Cu_{60}Zr_{40}$ binary amorphous alloy, the addition of Ti leads to a significant decrease in ΔT_x as well as in T_g and T_x, accompanying the change in the crystallization mode from the single stage to two or three stages. A similar compositional dependence is also recognized for the Cu–Hf–Ti alloy as shown in Fig. 4. However, T_x in the alloy system shows a maximum at 5 at.% Ti, though T_g decreases monotonously, leading to a maximum ΔT_x of 78 K at 5 at.% Ti, followed by a decrease in ΔT_x with further increases in Ti content.

It is expected that the decrease in T_g and T_x by the

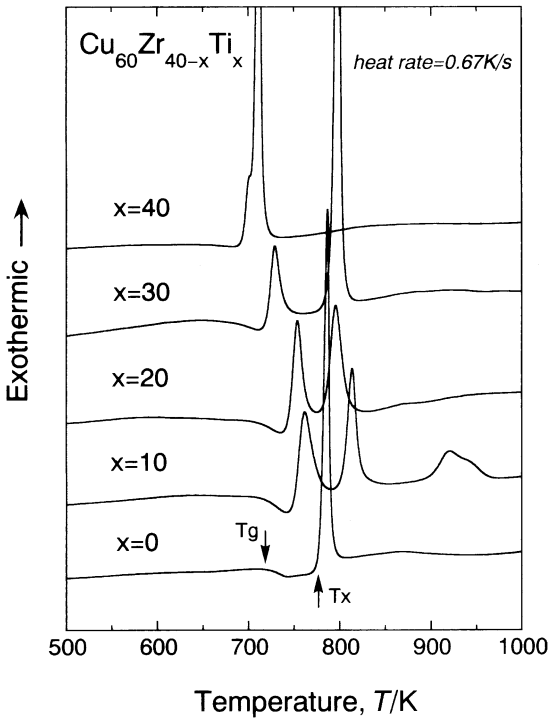

Fig. 3. DSC curves of melt-spun $Cu_{60}Zr_{40-x}Ti_x$ (x = 0–40 at.%) glassy alloys.

addition of Ti is related to the decrease in the melting temperature of the $Cu_{60}Zr_{40-x}Ti_x$ and $Cu_{60}Hf_{40-x}Ti_x$ alloys. Figures 5 and 6 show the DTA curves of the $Cu_{60}Zr_{40-x}Ti_x$ and $Cu_{60}Hf_{40-x}Ti_x$ (x = 0–40 at.%) alloys, respectively. The endothermic peak due to melting is seen for all the alloys and the melting reaction appears to occur through a single stage for the $Cu_{60}Zr_{40}$ and $Cu_{60}Zr_{20}Ti_{20}$ alloys as well as for $Cu_{60}Hf_{40}$ and $Cu_{60}Hf_{20-30}Ti_{10-20}$. Based on the data shown in Figs 5 and 6, the T_l and reduced glass transition temperature (T_g/T_l) were plotted as a function of Ti content for the $Cu_{60}Zr_{40-x}Ti_x$ and $Cu_{60}Hf_{40-x}Ti_x$ alloys in Fig. 7. The use of T_g/T_l is based on previous data [20, 21] that the glass-forming ability is more closely related to T_g/T_l rather than T_g/T_m. It is clearly seen that T_l shows a minimum value of 1127 K for $Cu_{60}Zr_{20}Ti_{20}$ and 1175 K for $Cu_{60}Hf_{20}Ti_{20}$. As a result, the 20 at.% Ti alloys exhibit a maximum T_g/T_l value of 0.63 and 0.62, respectively. There is no difference in the compositional dependence of T_g and T_g/T_l as well as in the absolute value of T_g/T_l. Here, it is noticed that the high T_g/T_l values exceeding 0.62 are obtained for the $Cu_{60}Zr_{20-30}Ti_{10-20}$ and $Cu_{60}Hf_{20-30}Ti_{10-20}$ glassy alloys. Considering that a number of bulk glassy alloys are obtained for the alloys with high T_g/T_l values above 0.60 by the copper mold casting method [10–12, 22], it is strongly expected that Cu-based bulk glassy alloys are formed by choosing the alloy compositions of $Cu_{60}Zr_{40-x}Ti_x$ and $Cu_{60}Hf_{40-x}Ti_x$ (x = 10–20%).

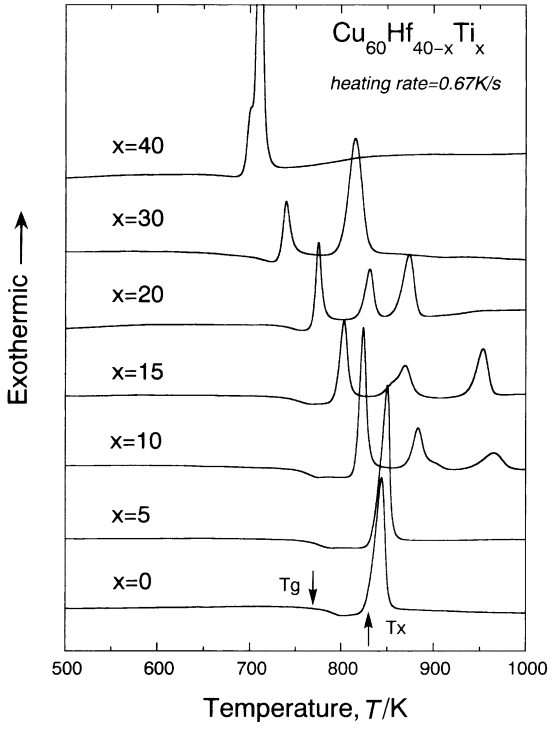

Fig. 4. DSC curves of melt-spun $Cu_{60}Hf_{40-x}Ti_x$ (x = 0–40 at.%) glassy alloys.

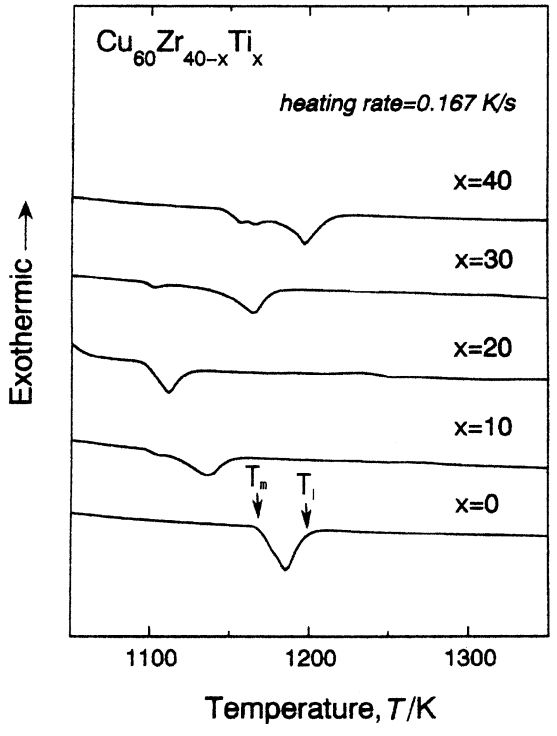

Fig. 5. DTA curves of the $Cu_{60}Zr_{40-x}Ti_x$ (x = 0–40 at.%) glassy alloys.

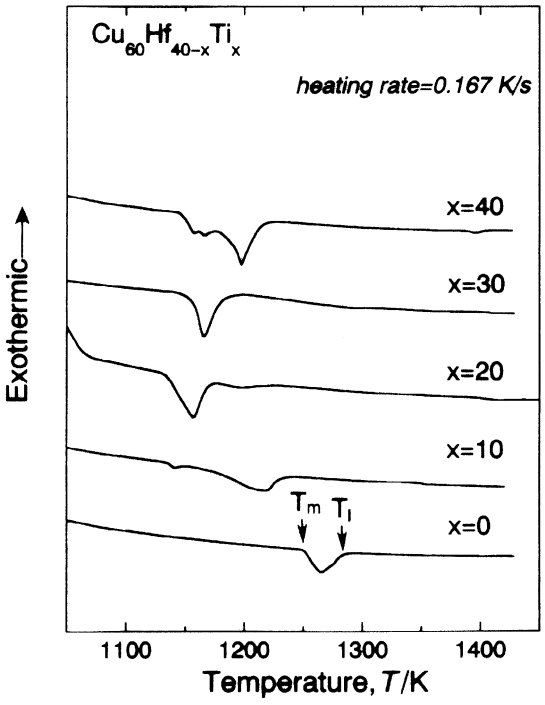

Fig. 6. DTA curves of the $Cu_{60}Hf_{40-x}Ti_x$ (x = 0–40 at.%) glassy alloys.

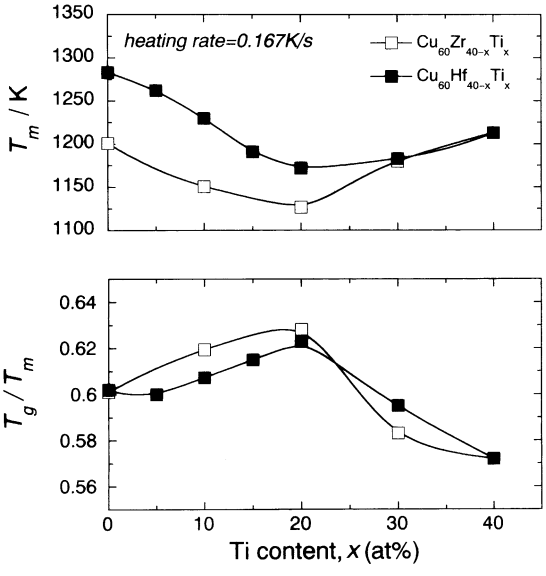

Fig. 7. Liquid temperature (T_l) and reduced glass transition temperature (T_g/T_l) as a function of Ti content for the $Cu_{60}Zr_{40-x}Ti_x$ and $Cu_{60}Hf_{40-x}Ti_x$ glassy alloys.

3.2. Formation of bulk glassy alloys

Figure 8 shows the X-ray diffraction patterns of the cylindrical $Cu_{60}Zr_{30}Ti_{10}$ and $Cu_{60}Hf_{25}Ti_{15}$ rods with diameters of 3 and 4 mm, together with the data of the melt-spun glassy ribbons. No distinct crystalline peaks are seen for the 3 and 4 mm samples in both the systems, indicating the formation of a glassy phase without crystallinity in the diameter range up

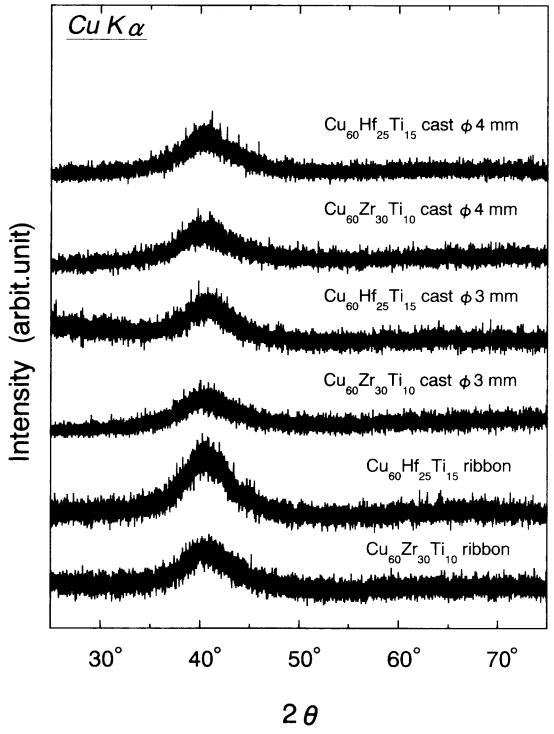

Fig. 8. X-ray diffraction patterns of cast $Cu_{60}Zr_{30}Ti_{10}$ and $Cu_{60}Hf_{25}Ti_{15}$ rods with diameters of 3 and 4 mm. The data of the melt-spun glassy alloy ribbons are also shown for comparison.

to 4 mm. In the DSC curves obtained from the cast glassy Cu–Zr–Ti and Cu–Hf–Ti alloy rods with diameters of 3 and 4 mm, we have also confirmed that T_g, T_x and heat of crystallization are nearly the same among the bulk and ribbon samples, being consistent with the results obtained from X-ray diffraction. As an example, the outer surface appearance of the cast bulk glassy rods with diameters of 3 and 4 mm is shown in Fig. 9. These rod samples exhibit good metallic luster and no appreciable concave due to a crys-

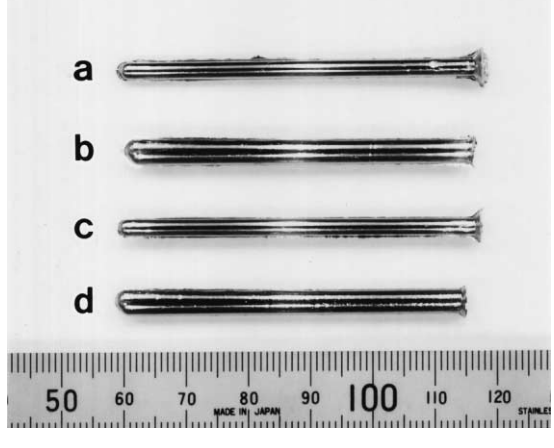

Fig. 9. Shape and outer surface appearance of cast $Cu_{60}Zr_{30}Ti_{10}$ (a, b) and $Cu_{60}Hf_{25}Ti_{15}$ (c, d) glassy rods with diameters of 3 and 4 mm.

talline phase is recognized. We have also confirmed the absence of a crystalline phase in the optical micrographs taken from the central region of the transverse cross section of the 3 and 4 mm rod samples. Here, it is important to point out that further increases in the sample diameter results in the formation of crystalline phases and hence the critical diameter of the ternary $Cu_{60}Zr_{30}Ti_{10}$ and $Cu_{60}Hf_{25}Ti_{15}$ alloys lies between 4 and 5 mm.

3.3. Mechanical properties of bulk glassy alloy rods

Figure 10 shows the compressive stress–elongation curves of the cast bulk glassy $Cu_{60}Zr_{30}Ti_{10}$ and $Cu_{60}Hf_{25}Ti_{15}$ rods with a diameter of 2 mm. It is seen that the glassy alloy rods exhibit elastic elongation in the elongation range up to 1.7%, followed by plastic elongation of about 1.6% and then final fracture, indicating that the new Cu-based bulk glassy alloys have rather good ductility. The Young's modulus (E), yield strength ($\sigma_{c,y}$) and fracture strength ($\sigma_{c,f}$) are 114 GPa, 1785 MPa and 2150 MPa, respectively, for the 30% Zr alloy and 124 GPa, 2010 MPa and 2160 MPa, respectively, for the 25% Hf alloy. The fracture takes place along the maximum shear plane which is declined by about 54° to the direction of the applied load and the fracture surface consists of a well-developed vein pattern typical of Zr-based bulk glassy alloys with good ductility [10–12], as shown in Fig. 11. A similar high fracture strength was also obtained in the tensile deformation mode. Figure 12 shows the tensile stress–elongation curves of the cast bulk $Cu_{60}Zr_{30}Ti_{10}$ and $Cu_{60}Hf_{25}Ti_{15}$ alloy sheets. The use of the sheet form samples is due to an ease of the sample preparation by electrical discharge machining. The tensile specimen has a gauge dimension of 1 mm in thickness, 2 mm in width and 10 mm in length. The Young's modulus (E), tensile yield strength ($\sigma_{t,y}$), tensile fracture strength ($\sigma_{t,f}$) and fracture elongation including elastic elongation ($\varepsilon_{t,f}$) are 112 GPa, 1780 MPa, 2000 MPa and 1.9%, respectively, for the former alloy sheet and 120 GPa, 1920 MPa, 2130 MPa and 2.0%, respectively, for the latter alloy sheet. The tensile fracture also takes place along the maximum shear plane and the developed vein pattern is seen over the whole fracture surface. Furthermore, the Vickers hardness (H_v) was measured to be 660 for $Cu_{60}Zr_{30}Ti_{10}$ and 670 for $Cu_{60}Hf_{25}Ti_{15}$. Here, it is important to describe that the tensile fracture strength is nearly the same as the compressive fracture strength, indicating good ductility of the Cu-based bulk glassy alloys. There have been no data on high-strength Cu-based bulk alloys with high strength above 2000 MPa in crystalline and glassy states [10–12, 23]. However, it is known that the Cu whisker with perfect crystal structure exhibits a high strength of 1700–2900 MPa [24]. It is particularly noticed that the tensile strength of the present bulk glassy alloy is comparable to that for the Cu whisker in spite of the much larger dimension of the specimen. In addition, the high strength level, exceeding largely 2000 MPa, has not been obtained for the Zr-based bulk glassy alloys in Zr–Al–Ni–Cu, Zr–(Ti,Nb,Ta)–Al–Ni–Cu and Zr–Ti–Be–Ni–Cu systems [10–12, 22]. Consequently, the present Cu-based bulk glassy alloys are expected to be developed as a new type of bulk structural material with higher strength combined with good ductility.

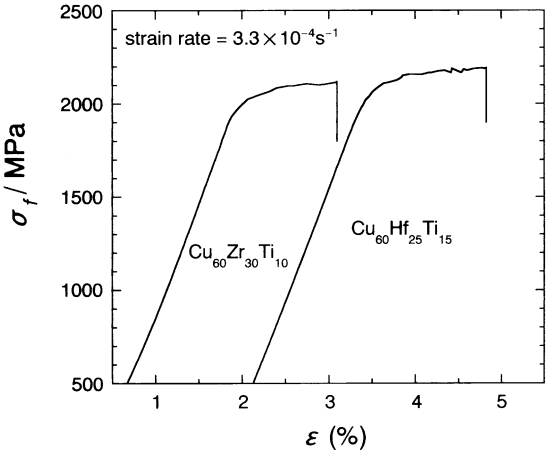

Fig. 10. Compressive stress–elongation curves of cast $Cu_{60}Zr_{30}Ti_{10}$ and $Cu_{60}Hf_{30}Ti_{10}$ glassy rods with a diameter of 2 mm.

4. DISCUSSION

As described above, the maximum sample diameter (d_m), ΔT_x and T_g/T_l are 4 mm, 37 K and 0.62, respectively, for $Cu_{60}Zr_{30}Ti_{10}$ and 4 mm, 60 K and 0.62, respectively, for $Cu_{60}Hf_{25}Ti_{15}$. On the other hand, ΔT_x and T_g/T_l of the $Cu_{60}Zr_{40}$ and $Cu_{60}Hf_{40}$ glassy alloys are 43–55 K and 0.60, respectively, and the critical sample diameter is about 1 mm. The relation between ΔT_x, T_g/T_l and maximum sample thickness for the ternary and binary glassy alloys indicates that the glass-forming ability is not directly related to ΔT_x but depends strongly on T_g/T_l. The present result indicates that the high glass-forming ability of the Cu-based alloys is obtained in the alloy compositions with high T_g/T_l values. The search for an appropriate element leading to a further decrease in T_l is important for future development of Cu-based bulk glassy alloys with larger diameters.

Next, we discuss the reason for the absence of the close correlation between ΔT_x and glass-forming ability. It has been reported that the high glass-forming ability leading to the formation of a bulk glassy alloy is obtained in the multicomponent alloy systems with the following three empirical rules [10–12]: (1) multicomponent system consisting of more than three elements, (2) significant atomic size mismatches above 12%, and (3) suitable negative heats of mixing. In the Cu–Zr–Ti and Cu–Hf–Ti systems, the atomic sizes change in the order of Zr>Ti>Cu and Hf>Ti>Cu and the atomic size ratios are 1.10 for Zr/Ti, 1.14 for Ti/Cu and 1.08 for Hf/Ti [25]. In

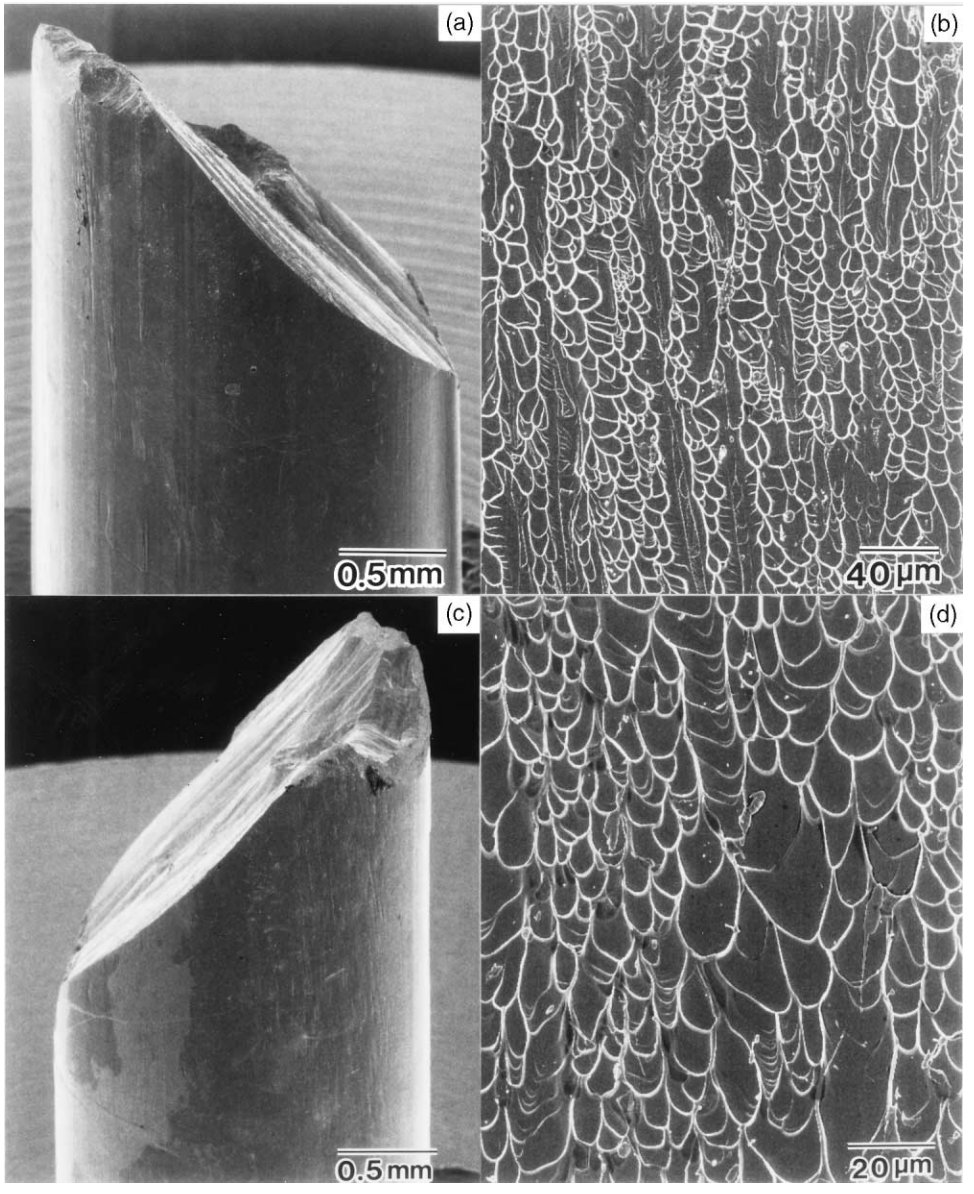

Fig. 11. Fracture surface of the cast $Cu_{60}Zr_{30}Ti_{10}$ (a, b) and $Cu_{60}Hf_{25}Ti_{15}$ (c, d) glassy rods subjected to fracture under compressive deformation mode.

addition, the heats of mixing have been estimated to be −23 kJ/mol for Cu–Zr, −9 kJ/mol for Cu–Ti, −17 kJ/mol for Cu–Hf, 0 kJ/mol for Zr–Ti and Hf–Ti [26]. These data on the atomic size ratios and the heats of mixing imply that the present Cu-based alloys do not perfectly satisfy the three empirical rules. The insufficient condition is thought to result in a significant decrease in ΔT_x through the reduction of the nucleation barrier for crystallization or the decrease of the driving force for crystallization for the Cu–Zr–Ti ternary alloys, though the glass-forming ability increases with a reduction in T_l. In addition, the largest value of T_g/T_m was obtained for the $Cu_{60}Zr_{20}Ti_{20}$ and $Cu_{60}Hf_{20}Ti_{20}$ alloys, while the bulk glassy alloy with the largest diameter was obtained in the compositions of $Cu_{60}Zr_{30}Ti_{10}$ and $Cu_{60}Hf_{25}Ti_{15}$, the ΔT_x values of which are larger than those for $Cu_{60}Zr_{20}Ti_{20}$ and $Cu_{60}Hf_{20}Ti_{20}$ alloys. The alloy compositions with the largest ΔT_x, with the highest T_g/T_l and with the maximum sample diameter are all different, which indicates that ΔT_x as well as T_g/T_l are important parameters for the formation of bulk glassy alloys. The present study indicates that the search for an element leading to an extension of the supercooled liquid region as well as a decrease in T_l may lead to finding a bulk glassy alloy with a much larger diameter, even in Cu-based alloy systems.

It is shown in Fig. 13 that the Cu–Zr–Ti and Cu–Hf–Ti bulk glassy alloys exhibit high tensile fracture strengths of 2000–2150 MPa. These values are comparable to that (2000 MPa) for a Cu whisker of 1 μm in diameter with perfect crystal structure [24] and

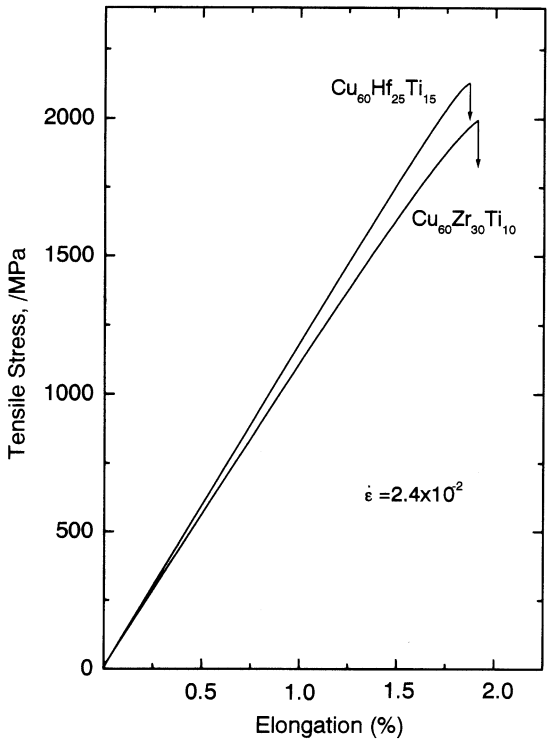

Fig. 12. Tensile stress–elongation curves of cast $Cu_{60}Zr_{30}Ti_{10}$ and $Cu_{60}Hf_{25}Ti_{15}$ glassy sheets with a thickness of 1 mm.

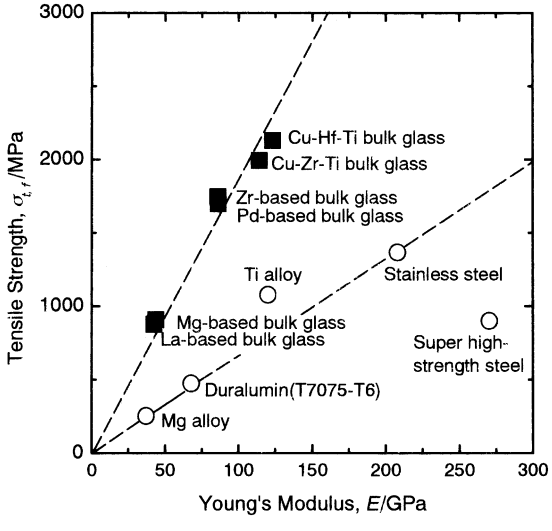

Fig. 13. Relation between Young's modulus (E) and tensile fracture strength ($\sigma_{t,f}$) for the cast $Cu_{60}Zr_{30}Ti_{10}$ and $Cu_{60}Hf_{25}Ti_{15}$ glassy sheets. The data of other bulk glassy alloys and conventional crystalline alloys are also shown for comparison.

much higher than those (1600–1700 MPa) [10–12, 22] for Zr-based bulk glassy alloys of Zr–Al–Ni–Cu, Zr–(Ti,Nb)–Al–Ni–Cu and Zr–Ti–Be–Ni–Cu systems. Here, we discuss the reason for the extremely high tensile fracture strength for the Cu-based bulk glassy alloy. Figure 13 summarizes the relations between E and $\sigma_{t,f}$ for the $Cu_{60}Zr_{30}Ti_{10}$ and $Cu_{60}Hf_{25}Ti_{15}$ bulk glassy alloys, together with the data of other bulk glassy alloys [12]. There is a clear tendency for E to increase with an increase in $\sigma_{t,f}$ for all the bulk glassy alloys. The slope in the linear relation for the bulk glassy alloys is also significantly different from that for the conventional crystalline alloys. It is characterized that the bulk glassy alloys have lower Young's modulus, larger elastic elongation limit and higher strength compared with those for the conventional crystalline alloys. It has been pointed out that the T_g and T_l of glassy alloys reflect the degree of bonding force among the constituent elements [27]. As shown in Table 1, T_g and T_l are the highest for the Cu–Hf–Ti ternary glassy alloys, followed by the Cu–Zr–Ti glassy alloys and then Zr–Al–Ni–Cu glassy alloys. The higher values of T_g and T_l allow us to presume that the bonding forces among Cu, Ti, Zr or Hf elements are stronger than those among Zr, Al, Ni and Cu elements. In addition, the relations between $\sigma_{t,f}$ and T_g or T_l for the Cu–Zr–Ti, Cu–Hf–Ti and Zr–Al–Ni–Cu bulk glassy alloys are shown in Fig. 14. Although some scatterings are seen, one can recognize a strong correlation, which demonstrates the appropriateness of the previous concept between strength and T_g or T_l.

5. SUMMARY

We have searched for a new Cu-based bulk glassy alloy with good mechanical properties which can be produced by the copper mold casting methods. The results obtained are summarized as follows.

1. In the $Cu_{60}Zr_{40-x}Ti_x$ and $Cu_{60}Hf_{40-x}Ti_x$ alloy systems, T_g and T_x tend to decrease with increasing Ti content, while T_l shows a minimum at around 20 at.% Ti. The resulting ΔT_x decreases gradually from 55 to 31 K for the former system and from 78 to 28 K for the latter system and the glass transition disappears for $Cu_{60}Ti_{40}$.
2. T_g/T_l shows a maximum phenomenon in the vicinity of 20 at.% Ti for the two alloy systems and the highest value reaches as much as 0.63.
3. The bulk glassy alloys are formed in the ternary systems and the largest diameter is 4 mm for the $Cu_{60}Zr_{30}Ti_{10}$ and $Cu_{60}Hf_{25}Ti_{15}$ alloys. The bulk glass-forming ability is more closely related to T_g/T_l values rather than ΔT_x.
4. The bulk glassy alloys possess good mechanical properties, i.e., Young's modulus of 114–134 GPa, compressive yield strength of 1785–2010 MPa, compressive fracture strength of 2150–2160 MPa, tensile yield strength of 1780–1920 MPa, tensile fracture strength of 2000–2130 MPa, elastic elongation of 1.5–2.0% and compressive plastic elongation of 0.8–1.7%. The combination of high glass-forming ability and good mechanical properties for the Cu-based alloys indicates the possibility of developing a new type of bulk structural material.

Table 1.

Alloys	T_g, T/K	T_x, T/K	ΔT_x, T/K	T_m, T/K	T_g/T_m
$Zr_{55}Al_{10}Ni_5Cu_{30}$	690	775	85	1113	0.62
$Zr_{60}Al_{10}Ni_{10}Cu_{20}$	676	770	94	1095	0.62
$Cu_{60}Zr_{30}Ti_{10}$	713	750	37	1153	0.62
$Cu_{60}Zr_{20}Ti_{20}$	708	743	35	1123	0.63
$Cu_{60}Hf_{30}Ti_{10}$	725	785	60	1170	0.62
$Cu_{60}Hf_{25}Ti_{15}$	730	795	65	1160	0.63

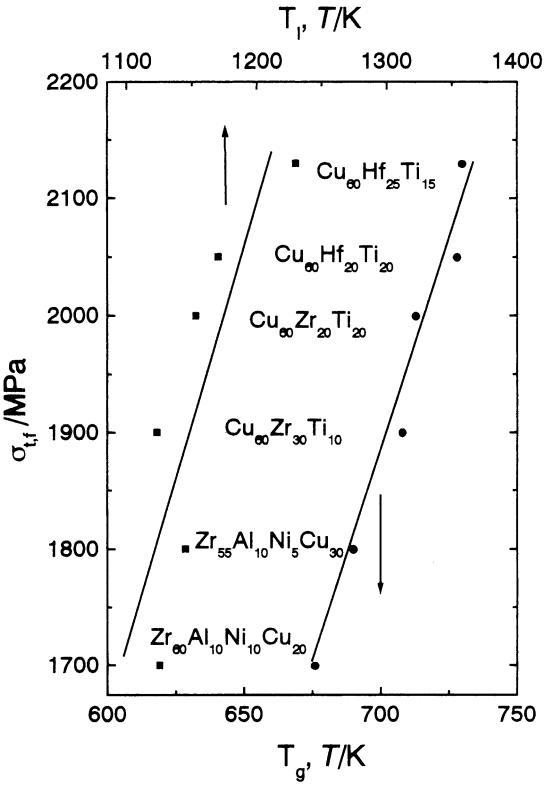

Fig. 14. Relation between tensile fracture strength ($\sigma_{t,f}$) and glass transition temperature (T_g) or liquid temperature (T_l) for the cast $Cu_{60}Zr_{30}Ti_{10}$ and $Cu_{60}Hf_{25}Ti_{15}$ glassy sheets. The data of the cast Zr–Al–Ni–Cu glassy alloys are also shown for comparison.

REFERENCES

1. Inoue, A., Zhang, T. and Masumoto, T., *Mater. Trans., JIM*, 1989, **30**, 965.
2. Inoue, A., Kato, A., Zhang, T., Kim, S. G. and Masumoto, T., *Mater. Trans., JIM*, 1991, **32**, 609.
3. Inoue, A., Zhang, T. and Masumoto, T., *Mater. Trans., JIM*, 1990, **31**, 177.
4. Peker, A. and Johnson, W. L., *Appl. Phys. Lett.*, 1993, **63**, 2342.
5. Inoue, A., Zhang, T., Nishiyama, N., Ohba, K. and Masumoto, T., *Mater. Lett.*, 1994, **19**, 131.
6. Inoue, A. and Gook, G. S., *Mater. Trans., JIM*, 1995, **36**, 1180.
7. Inoue, A., Nishiyama, N. and Matsuda, T., *Mater. Trans., JIM*, 1996, **37**, 181.
8. Wang, X. M. and Inoue, A., *Mater. Trans., JIM*, 2000, **41**, 539.
9. Itoi, T. and Inoue, A., *Mater. Trans., JIM*, 1999, **41**, 1256.
10. Inoue, A., *Mater. Trans., JIM*, 1995, **36**, 866.
11. Inoue, A., *Mater. Sci. Eng.*, 1997, **A226-228**, 357.
12. Inoue, A., *Acta mater.*, 2000, **48**, 279.
13. Lin, X. H. and Johnson, W. L., *J. Appl. Phys.*, 1995, **78**, 6514.
14. Zhang, T. and Inoue, A., *Mater. Trans., JIM*, 1999, **40**, 301.
15. Li, C., Saida, J., Kiminami, M. and Inoue, A., *J. Non-Cryst. Solids*, 2000, **261**, 108.
16. Inoue, A., Zhang, W., Zhang, T. and Kurosaka, K., *Mater. Trans.*, in press.
17. Inoue, A. and Makabe, E., Japanese Patent, 3011904.
18. Kakiuchi, H., Inoue, A., Onuki, M., Takano, Y. and Yamaguchi, T., *Mater. Trans.*, 2001, **43**(4), in press.
19. Inoue, A., Suryanarayana, C. and Masumoto, T., *J. Mater. Sci.*, 1981, **16**, 1391.
20. Li, Y., Ng, S. C., Ong, C. K., Hng, H. H. and Goh, T. T., *Scripta mater.*, 1997, **36**, 783.
21. Lu, Z. P., Tan, H. and Li, Y., *Mater. Trans., JIM*, 2000, **44**, 1397.
22. W. L. Johnson, C. T. Liu and A. Inoue, (ed.), *Bulk Metallic Glasses*. MRS, Warrendale 1999.
23. *Annual Book of ASTM Standards*. ASTM, West Conshohocken, 1997, p. 773.
24. Bokshtein, S. Z., Kishkin, S. T. and Svetlov, I. L., *Soviet Phys. Solid State*, 1963, **4**, 1272.
25. Wells, A. F., *Structural Inorganic Chemistry*. Oxford University Press, Oxford, 1984, p. 1382.
26. Boer, F. R., Boom, R., Mattens, W. C. M., Miedema, A. R. and Niessen, A. K., *Cohesion in Metals*. North-Holland, Amsterdam, 1988.
27. Chen, H. S., *Rep. Prog. Phys.*, 1980, **43**, 353.